Journal of Sol-Gel Science and Technology
https://doi.org/10.1007/s10971-018-4778-8

ORIGINAL PAPER: SOL-GEL AND HYBRID MATERIALS FOR ENERGY, ENVIRONMENT AND BUILDING APPLICATIONS

From sol–gel prepared porous silica to monolithic porous Mg_2Si/MgO composite materials

N. Hayati-Roodbari[1] · R. J. F. Berger[1] · J. Bernardi[2] · S. Kinge[3] · N. Hüsing[1] · M. S. Elsaesser[1]

Received: 9 February 2018 / Accepted: 7 August 2018

Abstract

Mg_2Si is apart from its conductivity properties expected to be a promising candidate for thermoelectric applications due to its low toxicity, low costs, and the high abundance of its precursor chemicals. Through the addition of a homogeneous distribution of nanoparticles (e.g. MgO) and by reducing the size of Mg_2Si to the nanometer regime, it is possible to decrease the thermal conductivity by increasing phonon-interface scattering and, as a result, improve the thermoelectric properties. However, classical approaches do not allow for the synthesis of nanocomposites from Mg_2Si and MgO. In this work, a straightforward route is presented towards homogeneously mixed Mg_2Si/MgO via a two-step magnesiothermic reduction process starting from sol–gel derived hierarchically organized porous silica. Monolithic materials composed of Mg_2Si and MgO in variable molar ratios are built up from a macroporous network of Mg_2Si with homogeneously distributed MgO particles exhibiting a crystallite size in the range of 24–37 nm.

Graphical Abstract

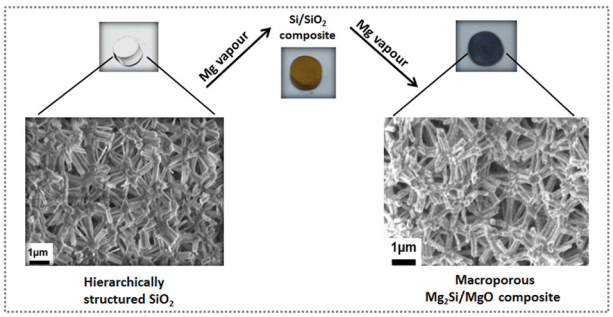

A versatile method, starting from hierarchically structured silica, to prepare Mg_2Si/MgO composite materials with an adjustable molar ratio of both components is shown. The morphology of the final product consists out of nanosizedMgO particles with crystallite sizes in the range of 30 nm embedded, and homogeneous distributed, in a macroporous Mg_2Si network.

Electronic supplementary material The online version of this article (https://doi.org/10.1007/s10971-018-4778-8) contains supplementary material, which is available to authorized users.

✉ M. S. Elsaesser
michael.elsaesser@sbg.ac.at

[1] Materials Chemistry, Paris Lodron University Salzburg, Jakob-Haringer Straße 2a, 5020 Salzburg, Austria

[2] USTEM, Technische Universität Wien, 1040 Vienna, Austria

[3] Toyota Motors Company Europe, 2000 Antwerp, Belgium

Published online: 21 August 2018

Highlights

- We present a new and versatile method to prepare macroporous Mg_2Si/MgO composites.
- Both components, Mg_2Si and MgO, are homogeneously distributed in the final composite.
- Our approach can easily be extended to other highly porous silica templates.
- The Mg_2Si/MgO network comprises nanosized MgO particles in a 3D interconnected Mg_2Si network.

Keywords Hierarchically structured silica · Nanocomposite material · Magnesiothermic reduction · Magnesium silicide

1 Introduction

Mg_2Si is the only intermetallic alloy formed in the Mg-Si system (Eq. 1) [1]. In recent years, it has attracted an increasing amount of interest for a wide range of applications in various fields, such as thermoelectrics and optics and in lithium-ion batteries, largely due to its low toxicity, unique optical and electrical properties, low costs of production, and environmental compatibility [2–8].

$$2Mg + Si \rightarrow Mg_2Si \quad (1)$$

It has been proven that nanostructuring of materials for thermoelectric applications, e.g., as nanofibres, results in improved performances compared to their bulk counterparts [9, 10]. Nanostructured thermoelectric materials are designed to introduce nanometer-sized polycrystallites and interfaces into bulk materials, which can improve the figure of merit ZT[1] for thermoelectric materials [11–14].

Adding a second phase, such as a metal oxide, into the system also reduces the lattice thermal conductivity by enabling an additional scattering mechanism and thus, improving thermoelectric performance [15, 16]. Cederkrantz et al. [17] investigated the influence of the addition of TiO_2 nanoparticles to Mg_2Si grains of > 100 nm on the thermoelectric properties of the latter. The addition of only 1 vol% TiO_2 nanoparticles to Mg_2Si resulted in a significant improvement of ZT at 300 °C, reaching ZT values of 0.042. This is a factor 2.75 higher than for pure Mg_2Si at the same temperature. Similar effects can be expected from using MgO instead of TiO_2 as a dielectric component in Mg_2Si, which seems to be easily achievable through magnesiothermic reduction of silica with an excess of magnesium (see equations 2 and 3). This has been shown by Szczech et al. [18] who converted diatomaceous earth particles to Mg_2Si/MgO composite powders via a gas-solid displacement reaction with magnesium vapor. Not only the micrometer sized morphology of the diatoms was preserved, but both components were also homogeneously mixed with MgO crystallites within a nanometer size range (~30 nm). This reaction represents a possible method for the production of large quantities of low-cost nanoscale thermoelectric materials with enhanced thermoelectric performance. Furthermore, for optimization of the thermoelectric performance an adjustment of the ratio of thermoelectric to dielectric phase is highly desirable [17].

$$SiO_2 + 2Mg \rightarrow Si + 2MgO \quad (2)$$

$$SiO_2 + 4Mg \rightarrow Mg_2Si + 2MgO \quad (3)$$

Nanostructured composites are typically fabricated by hot pressing or spark plasma sintering of fine powders prepared by grinding, milling, or wet chemical processing [11]. Such an approach creates a large number of interfaces between neighboring nanoparticles, thereby improving the thermoelectric performance [19]. However, typical drawbacks of these methods are that (1) a deliberate tailoring of the nanostructure is difficult to achieve, (2) the reaction is often incomplete, and (3) the final product is often contaminated with side-products [20]. In a previous study, we showed that magnesiothermic reduction of porous, hierarchically organized silica produced similarly structured meso/macroporous silicon, which could be converted to monolithic porous magnesium silicide via a specifically designed set-up for the gas-solid displacement reaction [20].

In the present study, we have developed a two stage synthesis strategy to prepare monolithic Mg_2Si/MgO composite materials comprising a macroporous network and an adjustable ratio of both components. This approach opens a simple route towards a variety of Mg_2Si/MgO materials with respect to chemical composition and morphology compared to previously described processes [19]. By magnesiothermically reacting hierarchically structured macro/mesoporous silica with a low amount of Mg vapor, a mixture of Si and remaining silica is obtained. If this material is reacted with Mg vapor again a complete conversion to Mg_2Si and MgO is obtained according to the parallel reactions given in Eqs. 1 and 3. The overall process has the following advantages:

- Easily adjustable ratio of Mg_2Si and MgO
- Nanosized MgO particles homogeneously embedded in a macroporous Mg_2Si network

[1] ZT defined as dimensionless scalar: $ZT = S^2 \rho^{-1} \kappa^{-1} T$ with S (Seebeck coefficient), ρ (electrical resistivity), κ (thermal conductivity), and T (absolute temperature)

Table 1 Calculated amounts of reactants and content after magnesiothermic reduction of Si/SiO_2 composites

Sample	SiO_2 [mol]	Mg [mol]	Product SiO_2 [mol]	Product Si [mol]
Mg_2Si: MgO A1	1.00	0.50	0.75	0.25
Mg_2Si: MgO B1	1.00	1.12	0.44	0.56
Mg_2Si: MgO C1	1.00	1.61	0.20	0.80

Table 2 Calculated amounts of reactants and content after reaction of the Mg_2Si/MgO composites

Sample	SiO_2 [mol]	Si [mol]	Mg [mol]	Product Mg_2Si [mol]	Product MgO [mol]	Mg_2Si/MgO molar ratio
Mg_2Si: MgO A2	0.75	0.25	3.50	1.00	1.50	0.66
Mg_2Si: MgO B2	0.44	0.56	2.88	1.00	0.88	1.14
Mg_2Si: MgO C2	0.20	0.80	2.39	1.00	0.40	2.50

- Low equipment cost
- No further purification steps are required

2 Experimental procedure

2.1 Materials

Ethylene glycol (Sigma-Aldrich) was purified by drying over Na_2SO_4 (Prolabo) and filtering. Tetraethoxysilane (Merck), trimethylchlorosilane (TMCS, Sigma-Aldrich), Pluronic P123 ($EO_{20}PO_{70}EO_{20}$, BASF), petroleum ether (40–60 °C, Prolabo), magnesium powder (for synthesis, Merck), hydrochloric acid (37%, Merck), and acetic acid (glacial, Merck) were used without further purification.

2.2 Preparation of hierarchically organized silica

Hierarchically organized meso/macroporous silica (SiO_2) was prepared according to Brandhuber et al. by sol–gel processing of tetrakis(2-hydroxyethyl)orthosilicate (EGMS) combined with a templating approach in an aqueous medium containing Pluronic P123™ and 1 M hydrochloric acid (HCl), with a composition by weight of Si/P123/0.1 M HCl = 8.4/30/70 [21, 22]. The surface hydrophobization concomitant with surfactant extraction was performed by immersing the gel bodies in TMCS (10% in petroleum ether (PE)). After washing with PE three times, the wet silica gels were cut into small, monolithic slices (with 2–3 mm in height and 3–4 mm in diameter (c.f. Fig. 2)). After drying at 80 °C the slices were calcined at 550 °C for 4 h.

2.3 Reaction of SiO_2 with Mg with various molar ratios to obtain Mg_2Si/MgO or Si/SiO_2 composites

Magnesiothermic reduction [1, 23, 24] was performed using a "mesh-boat" set-up to ensure spatial separation of silica and Mg (see Fig. 2). The silica slices were placed on a stainless steel mesh with the magnesium powder beneath in a small boat, and together these were inserted into a stainless steel tube filled with an argon atmosphere. This was then placed in a tube furnace under a slight argon stream and heated to 650 °C with a heating rate of 1 K min^{-1} and 2 h holding time. In order to obtain Mg_2Si/MgO composites in a direct one-step reaction, silica and Mg were used in a molar ratio of 1:4. In this case no further purification treatment was performed. To prepare three different Si/SiO_2 composite materials for further treatment as described in "Synthesis of Mg_2Si/MgO composites" section, the amount of Mg was kept below 2 moles (0.50–1.61) in relation to SiO_2 (see detailed calculated values in Table 1 for samples A1, B1, and C1). Removal of the by-product (MgO) was conducted by immersing the reaction product in 1 mL of degassed water, followed by addition of 20 mL of 2 M hydrochloric acid and 10 mL of diluted acetic acid for 3 h at 40 °C. Afterwards, washing with degassed water was repeated until a neutral pH-value was achieved. The resulting brown monoliths were dried in vacuum.

2.4 Synthesis of Mg_2Si/MgO composites

To prepare three different Mg_2Si/MgO composite samples (A2, B2, and C2), the same set-up as described before was used. The silica/silicon monoliths (A1, B1, or C1) were placed on a mesh and separated from Mg powder in the boat beneath (see detailed amounts in Table 2). Afterwards, the set-up was placed in a stainless steel tube, which was heated in a tube furnace under argon atmosphere to 650 °C with 1 K min^{-1} heating rate and 2 h holding time.

3 Methods

Powder X-ray diffractograms (PXRD) were recorded using a Bruker D8 diffractometer with a DaVinci Design and

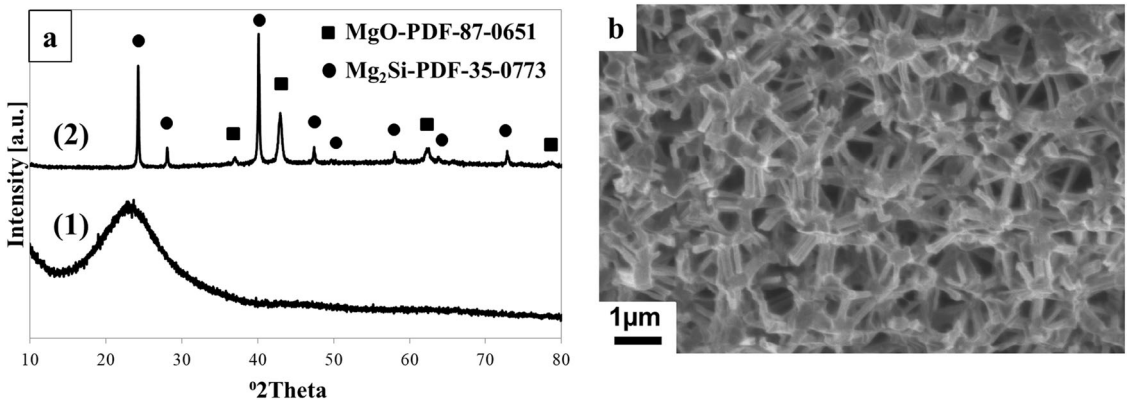

Fig. 1 PXRD pattern of **a** (1) hierarchically structured, amorphous silica and (2) Mg_2Si/MgO composite material after reaction at 650 °C for 2 h (molar ratio SiO_2/Mg 1:4); **b** SEM image of the Mg_2Si/MgO composite material of (2)

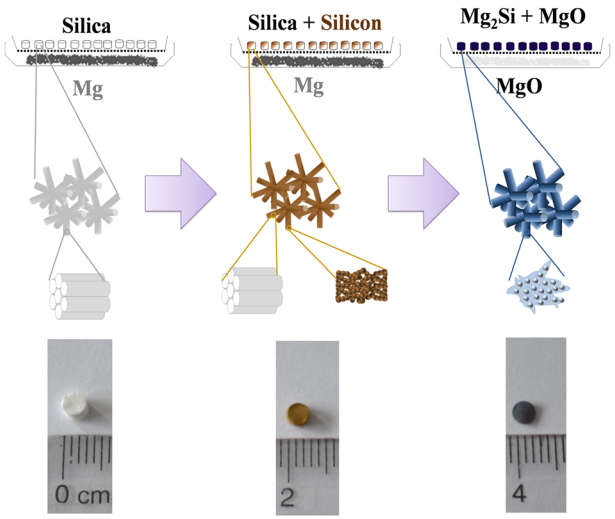

Fig. 2 Schematic presentation of the two-step process to yield a composite material with adjustable ratio of Mg_2Si/MgO (upper part); photographs of the precursor silica gel (bottom left), the Si/SiO_2 monolith (bottom middle) and the (Mg_2Si/MgO) monolith (bottom right)

CuK_α radiation. Evaluation of crystallite sizes was done according to the Scherrer equation and Rietveld refinement was performed using TOPAS V4-2 software (Bruker).

Sample morphology was examined using a Zeiss Ultra Plus scanning electron microscope (SEM) operated at an accelerating voltage of 2 kV with an in-lens detector. Silica samples were sputtered with gold to provide an electrically conductive surface. An Oxford Instruments X-Max energy dispersive X-ray (EDX) detector was used for elemental analysis.

The microstructure of the samples was studied with transmission electron microscopy (TEM) using a TECNAI F20 field emission microscope operated at an accelerating voltage of 200 kV. Images were recorded with a Gatan Orius SC 600 charge-coupled device (CCD) camera.

Nitrogen sorption isotherms were recorded at 77 K using a sorption porosimeter (Micromeritics, ASAP 2420). Prior to the measurement, samples were degassed for 3 h at 100 °C in vacuum. The Brunauer-Emmett-Teller (BET) surface area was evaluated using adsorption data in a relative pressure range p/p_0 0.05–0.25. The mesopore size distribution was calculated on the basis of the desorption branch using the Barrett–Joyner–Halenda (BJH) model.

4 Results and discussions

Based on the experiments by Szczech et al. [18] with diatomaceous earth SiO_2, and also on our own previous experiments [20], we reacted hierarchically structured silica, consisting of a cellular network comprising struts with hexagonally ordered mesopores with a diameter of 8 nm and a pore wall thickness of 3–5 nm (see Supplementary Fig. S1 ESI), directly with four moles of Mg vapor at a temperature of 650 °C for 2 h following Eq. 3. The PXRD pattern in Fig. 1b confirms the complete conversion to a Mg_2Si/MgO composite with a ratio of 44:56 by weight (molar ratio Mg_2Si/MgO = 0.41). Starting with amorphous silica, indicated by a very broad peak in the PXRD diffraction pattern at 22° 2 Theta (Fig. 1a), a product with crystallite sizes of 73 ± 5 nm (Mg_2Si) and 21 ± 5 nm (MgO) was obtained according to the Scherrer equation. Mg vapor can easily diffuse into and through the macroporous network, followed by condensation and reaction with the SiO_2 on the struts (see Supplementary Fig. S1 ESI), which are typically of about 1 µm in length and 100 nm in diameter. This build-up of a pure crystalline material upon the magnesiothermic conversion is accompanied by the destruction of pores in the mesoscopic range. However, a perfect preservation of the macroporous network of Mg_2Si/MgO is observed (see Fig. 1b). Similar results were obtained recently for the reaction of Si with Mg to yield pure Mg_2Si [20].

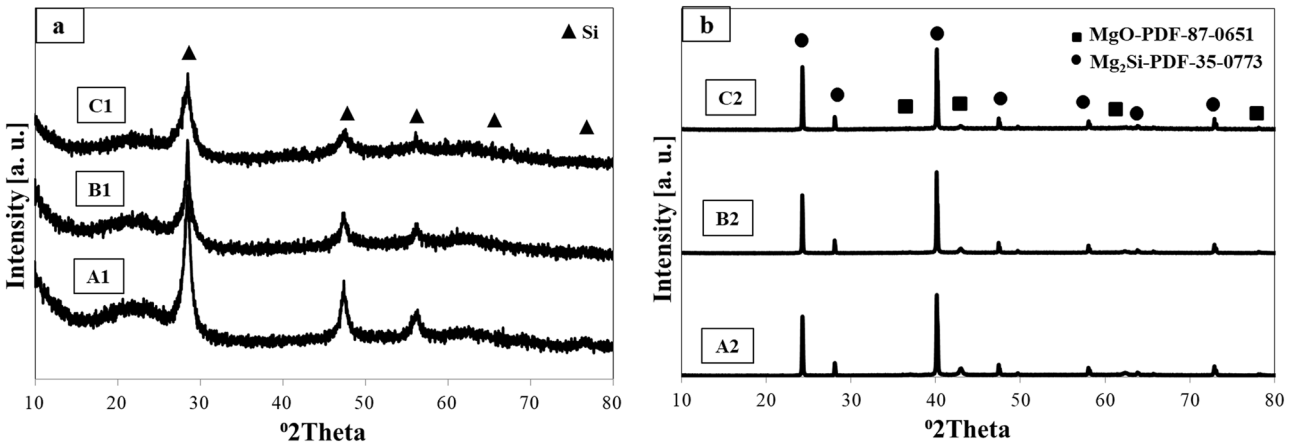

Fig. 3 **a** PXRD patterns of the intermediate silica/silicon product A1, B1, and C1; **b** PXRD patterns of the final Mg_2Si/MgO composite materials A2, B2, and C2

It is very likely that the presence of MgO mitigates the locally released heat from the exothermic reaction helping to preserve the macro-morphology [23]. Elemental analysis by EDX confirmed a homogeneous distribution of Mg_2Si and MgO in the macroporous network (see Supplementary Information, Fig. S2) again supporting the contention of the benefit of the better diffusion in a highly porous precursor material. The loss of mesopores is indicated by a decrease of the specific surface area (SSA) from 700 $m^2 g^{-1}$ in silica to less than 50 $m^2 g^{-1}$ in the composite sample. This data proves that we can successfully prepare a monolithic, but nanosized, Mg_2Si/MgO composite material via a direct one-step magnesiothermic reaction. However, any adjustment of the ratio of the components to each other does not seem to be possible. Variations in the amounts of Mg for the magnesiothermic reaction would result in either silica and/or silicon containing samples or residual unreacted Mg.

In order to gain better control over the molar ratio between Mg_2Si and MgO in the final composite material, we developed a route based on two successive magnesiothermic reductions making use of the two parallel reactions as given in Eqs. 1 and 3. The aim is to first convert silica with a very low amount of Mg to a silica/silicon composite material, which is reacted in a second step with Mg to give a Mg_2Si/MgO composite (see Fig. 2).

In principle, the reaction of silica and Mg is performed as described before with the exception that the amount of Mg is now adjusted to values lower than four moles (thus sub-stoichiometric with respect to Equation 2).

$$SiO_2 + (2-2x)Mg \rightarrow (1-x)Si + x\,SiO_2 + (2-2x)MgO \quad (4)$$

$$x_A = 0.75; x_B = 0.44; x_C = 0.20$$

$$(1-x)Si + (2-2x)Mg \rightarrow (1-x)Mg_2Si \quad (5a)$$

$$x\,SiO_2 + (2x)Mg \rightarrow (2x)MgO + xMg_2Si \quad (5b)$$

This leads to an incomplete reaction resulting in a monolithic material consisting of silicon, MgO and remaining silica. The given amount of Mg, indicated by "*x*" in Eq. 4, is always adjusted to < 2. In this series, the values have been set to (A, B, and C) $x_A = 0.75$; $x_B = 0.44$, $x_C = 0.20$, and thus the amount of Mg determines the content of residual silica. MgO is removed by HCl etching leaving a macroporous silicon/silica network behind. Although the distribution of Si and SiO_2 in this network is unknown, we conclude that it is homogeneous since it is homogeneously distributed in the final product (see Supplementary Information; EDX data in Fig. S3). MgO removal is necessary to be able to adjust the desired ratios in the final product. The dried Si/SiO_2 composite monolith is then subjected to a second reaction with Mg. The amount of Mg is calculated on the basis of the calculated ratios of Si/SiO_2 (see Table 1) and the stoichiometry given in Eqs. 5a and b. While silica is now converted to magnesium silicide and MgO (Eq. 5b), silicon directly gives magnesium silicide according to Eq. 5a. In this step, Si and SiO_2 form the final macroporous Mg_2Si network with homogeneously distributed MgO crystallites. Depending on the amount of silica in this step, a number of different compositions (A2, B2, and C2) are accessible without further purification (see also photographs in Fig. 2).

The monolithic shape of the starting silica gel is preserved upon all processing steps to the final composite material without significant shrinkage. As expected, the color change from white to slight brownish and furthermore to bluish demonstrates the transformation from silica to silicon/silica and Mg_2Si/MgO. Along with the transformation from silica to the Mg_2Si/MgO composite materials, we obtain a slight decrease in density overall: 0.35 g cm^{-3} for silica and 0.10–0.20 g cm^{-3} for Mg_2Si/MgO (A2 0.10; B2

Table 3 Product compositions of Mg_2Si/MgO composites

Samples	Product Mg_2Si [mol]	Product MgO [mol]	Mg_2Si crystallite size [nm]	MgO crystallite size [nm]	Mg_2Si/MgO molar ratio
Mg_2Si/MgO A2	0.76	1.17	193	37	0.65
Mg_2Si/MgO B2	0.78	0.69	241	29	1.13
Mg_2Si/MgO C2	0.85	0.35	269	24	2.45

Crystallite sizes were calculated by use of the Scherrer equation.

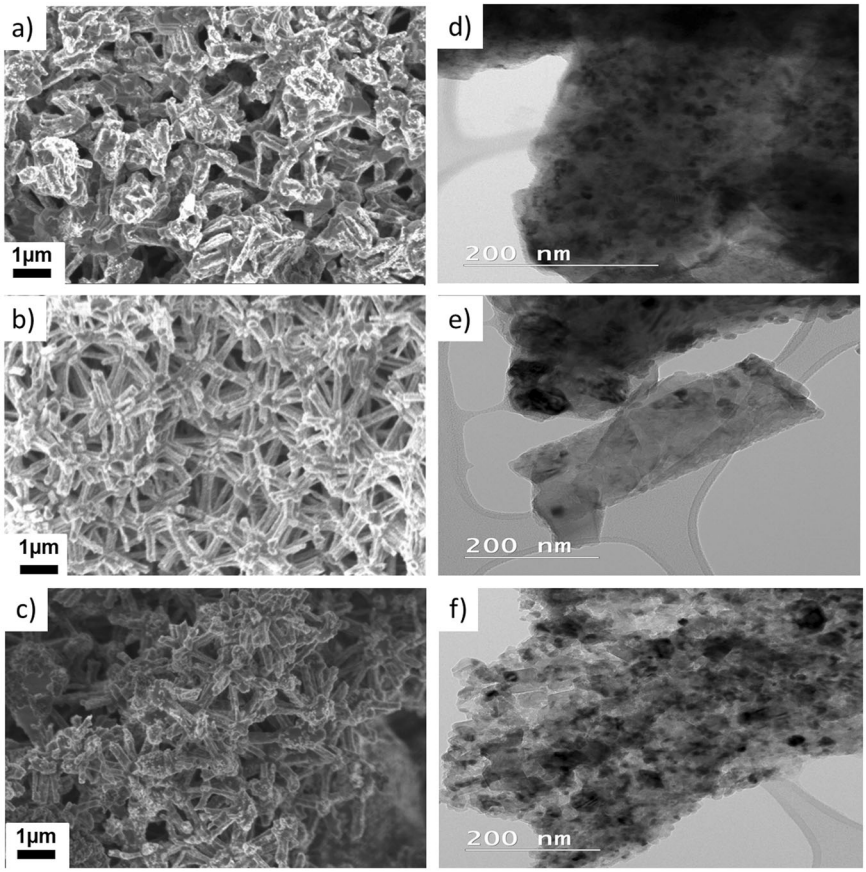

Fig. 4 SEM images of **a** Mg_2Si/MgO composite A2, **b** Mg_2Si/MgO composite B2, **c** Mg_2Si/MgO composite C2, and TEM images of **d** Mg_2Si/MgO composite A2, **e** Mg_2Si/MgO composite B2, **f** Mg_2Si/MgO composite C2

0.13; C2 0.20). Interestingly, the densities of the intermediate stage of Si and silica (after removal of MgO) are the lowest, with measured values of 0.067 g cm^{-3} for A1, 0.085 for B1, and 0.095 for C1. Considering the low densities of amorphous silica (~2.20 g cm^{-3}), silicon (2.32 g cm^{-3}) and Mg_2Si (1.99 g cm^{-3}) compared to MgO (3.58 g cm^{-3}), this is not unexpected.

To prove our concept we prepared three different samples with theoretical Mg_2Si/MgO ratios of 0.66, 1.14, and 2.50 indicated with A2, B2, and C2 (Table 2). For the first reaction, we reacted $(2-2x)$ mole of Mg and 1 mole of SiO_2, with $x = 0.20$, 0.44, and 0.75 being the amount of remaining silica after the first step. A detailed overview of the calculated reaction compositions is given in Table 2. Since Mg powder contains traces of MgO impurities we take advantage of the boat-mesh set-up, which ensures spatial separation from the reactants, since MgO always remains beneath the mesh. In addition, the chosen Ar atmosphere avoids formation of MgO traces due to Mg oxidation. We investigated the intermediate SiO_2/Si composites by PXRD diffraction as shown in Fig. 3a after extraction of MgO. All three samples (A1, B1, and C1) show an amorphous signal with a broad reflection at ~22° 2 Theta indicating remaining silica accompanied by Bragg reflexes for crystalline silicon. Unfortunately, the amorphous character of silica made detailed calculations of the composition by Rietveld refinement impossible.

The three Mg_2Si/MgO composite samples were characterized by PXRD diffraction (see Fig. 3b). For all three samples only Mg_2Si and MgO are present (reference pdf files: Mg_2Si-PDF-87-0651 and MgO-PDF-35-0773). For comparison, we normalized the XRD patterns and calculated the ratios of Mg_2Si and MgO by Rietveld refinement. As shown in Table 2, the obtained values for the molar ratio

between Mg_2Si and MgO match very well with the calculated contents of silica and Mg and show the great versatility and reliability of the method. Expectedly, the absolute experimental amounts obtained in the final product are lower than the theoretically calculated ones (c.f. Tables 2 and 3) due to material loss during washing, processing by use of the mesh or even handling. The crystallite sizes calculated by the Scherrer equation are in the range 193 to 269 nm (for Mg_2Si) and ~30 nm (for MgO) (see Table 2). The morphology of the obtained composite samples was investigated by SEM and TEM. Figure 4 shows the microstructure indicating in all cases a preservation of the macroporous cellular network. The TEM images in Fig. 4 reveal the fine dispersion of Mg_2Si and MgO crystallites in each strut with the absence of pores in the mesoscopic range, which proves the contention that Si and SiO_2 are also homogeneously distributed in the intermediate product. We examined the distribution of Mg_2Si and MgO also by EDX and obtained a homogeneous distribution in an area of several square µm of the sample (see Fig S3 ESI). The loss of mesopores during processing is also supported by nitrogen sorption analysis and very low SSAs ($< 50\ m^2\ g^{-1}$) in comparison to the highly porous silica precursor ($700\ m^2\ g^{-1}$).

5 Conclusion

In summary, we developed a facile and versatile method to prepare macroporous Mg_2Si and MgO composite materials with adjustable molar ratios of both components. Magnesiothermic reduction of hierarchically structured amorphous silica with an amount of Mg powder that results in an incomplete reaction produced silicon/silica composites. The latter could be reacted in a second treatment with Mg to give Mg_2Si/MgO composites. The ratio between magnesium silicide and magnesium oxide is easily controlled via the amount of Mg used in both reactions.

Both components are homogeneously distributed in the final product, implying good diffusion of Mg into the porous scaffolds of SiO_2 and Si/SiO_2. From a structural point of view, the monolithic shape as well as the macroporous network are preserved during the reactions with magnesium. Smaller mesopores, however, are lost in the reaction process. Both components Mg_2Si and MgO are obtained as crystalline materials with crystallite sizes in the upper nanometer regime (> 150 nm) and about 30 nm, respectively. Both reaction steps can be conducted in the same set-up.

As a broad variety of porous silica structures are available, this approach can easily extended to many other composite morphologies of Mg_2Si and MgO in different molar ratios. To overcome a low electrical conductivity of the porous composite material in thermoelectric applications, typically a sintering process (plasma sintering) is followed up to yield a bulk form with homogeneous distribution of MgO nano crystals.

Acknowledgements Open access funding provided by Paris Lodron University of Salzburg. The help of G. Tippelt for the X-ray diffraction measurements and M. Suljic for the N_2 sorption measurements is acknowledged. Financial support of Toyota Motors Company Europe is kindly appreciated.

Compliance with ethical standards

Conflict of interest The authors declare that they have no conflict of interest.

References

1. Chen K, Bao Z, Shen J, Wu G, Zhou B, Sandhage KH (2012) Freestanding monolithic silicon aerogels. J Mater Chem 22 (32):16196–16200. https://doi.org/10.1039/C2JM31662E
2. Yan JM, Huang HZ, Zhang J, Yang Y (2008) The study of Mg_2Si/carbon composites as anode materials for lithium ion batteries. J Power Sources 175(1):547–552. https://doi.org/10.1016/j.jpowsour.2007.06.074
3. Zhang C, Ni D, Liu Y, Yao H, Bu W, Shi J (2017) Magnesium silicide nanoparticles as a deoxygenation agent for cancer starvation therapy. Nat Nano advance online publication. https://doi.org/10.1038/nnano.2016.280
4. de Boor J, Saparamadu U, Mao J, Dahal K, Müller E, Ren Z (2016) Thermoelectric performance of Li doped, p-type Mg_2(Ge, Sn) and comparison with Mg_2(Si,Sn). Acta Mater 120:273–280. https://doi.org/10.1016/j.actamat.2016.08.057
5. De Boor J, Gloanec C, Kolb H, Sottong R, Ziolkowski P, Müller E (2015) Fabrication and characterization of nickel contacts for magnesium silicide based thermoelectric generators. J Alloy Compd 632:348–353. https://doi.org/10.1016/j.jallcom.2015.01.149
6. Santos-Peña J, Brousse T, Schleich DM (2000) Mg_2Si and MSi_2 (M=Ca, Fe) silicon alloys as possible anodes for lithium batteries. Ionics 6(1):133–138. https://doi.org/10.1007/BF02375557
7. Liu Y, He Y, Ma R, Gao M, Pan H (2012) Improved lithium storage properties of Mg_2Si anode material synthesized by hydrogen-driven chemical reaction. Electrochem Commun 25:15–18. https://doi.org/10.1016/j.elecom.2012.09.010
8. Shen Y (2017) Rice husk silica-derived nanomaterials for battery applications: A literature review. J Agric Food Chem 65(5):995–1004. https://doi.org/10.1021/acs.jafc.6b04777
9. Li GH, Gill HS, Varin RA (1993) Magnesium silicide intermetallic alloys. Metall Trans A 24(11):2383–2391. https://doi.org/10.1007/BF02646518
10. Biswas K, He J, Blum ID, Wu C-I, Hogan TP, Seidman DN, Dravid VP, Kanatzidis MG (2012) High-performance bulk thermoelectrics with all-scale hierarchical architectures. Nature 489 (7416):414–418. https://doi.org/10.1038/nature11439
11. Chen Z-G, Han G, Yang L, Cheng L, Zou J (2012) Nanostructured thermoelectric materials: Current research and future

challenge. Progress Nat Sci: Mater Int 22(6):535–549. https://doi.org/10.1016/j.pnsc.2012.11.011
12. Hicks LD, Dresselhaus MS (1993) Effect of quantum-well structures on the thermoelectric figure of merit. Phys Rev B 47 (19):12727–12731. https://doi.org/10.1103/PhysRevB.47.12727
13. Persson AI, Koh YK, Cahill DG, Samuelson L, Linke H (2009) Thermal conductance of InAs nanowire composites. Nano Lett 9 (12):4484–4488. https://doi.org/10.1021/nl902809j
14. Szczech JR, Higgins JM, Jin S (2011) Enhancement of the thermoelectric properties in nanoscale and nanostructured materials. J Mater Chem 21(12):4037–4055. https://doi.org/10.1039/C0JM02755C
15. Li J-F, Liu W-S, Zhao L-D, Zhou M (2010) High-performance nanostructured thermoelectric materials. NPG Asia Mater 2 (4):152–158. https://doi.org/10.1038/asiamat.2010.138
16. Chen L, Huang X, Zhou M, Shi X, Zhang W (2006) The high temperature thermoelectric performances of $Zr_{0.5}Hf_{0.5}Ni_{0.8}Pd_{0.2}Sn_{0.99}Sb_{0.01}$ alloy with nanophase inclusions. J Appl Phys 99(6):064305. https://doi.org/10.1063/1.2180432
17. Cederkrantz D, Farahi N, Borup KA, Iversen BB, Nygren M, Palmqvist A (2012) Enhanced thermoelectric properties of Mg_2Si by addition of TiO_2 nanoparticles. J Appl Phys 111(2):023701. https://doi.org/10.1063/1.3675512
18. Szczech JR, Jin S (2008) Mg_2Si nanocomposite converted from diatomaceous earth as a potential thermoelectric nanomaterial. J Solid State Chem 181(7):1565–1570. https://doi.org/10.1016/j.jssc.2008.04.020
19. Vineis CJ, Shakouri A, Majumdar A, Kanatzidis MG (2010) Nanostructured thermoelectrics: big efficiency gains from small features. Adv Mater 22(36):3970–3980. https://doi.org/10.1002/adma.201000839
20. Hayati-Roodbari N, Berger RJF, Bernardi J, Kinge S, Husing N, Elsaesser MS (2017) Monolithic porous magnesium silicide. Dalton Trans 46(27):8855–8860. https://doi.org/10.1039/C7DT00571G
21. Brandhuber D, Huesing N, Raab CK, Torma V, Peterlik H (2005) Cellular mesoscopically organized silica monoliths with tailored surface chemistry by one-step drying/extraction/surface modification processes. J Mater Chem 15(18):1801–1806. https://doi.org/10.1039/B417675H
22. Brandhuber D, Peterlik H, Hüsing N (2005) Simultaneous drying and chemical modification of hierarchically organized silica monoliths with organofunctional silanes. J Mater Chem 15(35-36):3896–3902. https://doi.org/10.1039/B505976C
23. Banerjee HD, Sen S, Acharya HN (1982) Investigations on the production of silicon from rice husks by the magnesium method. Mater Sci Eng 52(2):173–179. https://doi.org/10.1016/0025-5416(82)90046-5
24. Waitzinger M, Elsaesser MS, Berger RJF, Akbarzadeh J, Peterlik H, Hüsing N (2016) Self-supporting hierarchically organized silicon networks via magnesiothermic reduction. Mon für Chem - Chem Mon 147(2):269–278. https://doi.org/10.1007/s00706-015-1611-8